

# Computer Tomography System for Investigation of Translation Process of FRC Plasma on the FIX Device

SHINAGAWA Kazumasa<sup>1</sup>, YOSHIMURA Satoru, SUGIMOTO Satoshi, KITANO Katsuhisa,  
NAKAMURA Atsushi<sup>2</sup>, OKADA Shigefumi and GOTO Seiichi  
*Plasma Physics Laboratory, Graduate School of Engineering, Osaka University,  
Yamada-oka 2-1, Suita, Osaka 565-0871, Japan*

(Received: 11 December 2001 / Accepted: 6 September 2002)

## Abstract

A computer tomography system for the investigation of the translation process of the field reversed configuration (FRC) plasma was established on the FIX device. This system was composed of three arrays of detectors sensitive to the near-infrared radiation. To avoid the light reflection at the vacuum wall, black anodized aluminum panels were installed just inside the metal chamber. Two-dimensional distributions of the light emissivity of the translated FRC plasma were reconstructed using the Fourier–Bessel expansion technique. Our results indicated that the emission reached a maximum intensity when the FRC plasma was reflected by the mirror field, and also that the temporal evolution of the width of the reconstructed emission profile had the similar tendency to that of the separatrix radius during the translation.

## Keywords:

FRC, plasma, computer tomography, Fourier–Bessel expansion technique, translation

## 1. Introduction

The field reversed configuration (FRC) [1] is considered to be a promising candidate for the D-<sup>3</sup>He fusion reactor because of its high  $\beta$  value. Mostly, FRC plasmas are produced in theta pinch devices which consist of a quartz discharge tube and massive high voltage pinch coils. Therefore, the accessibility of the plasma to heating facilities is inexpedient and heating experiments of FRC plasmas have been scarcely carried out so far. On the FIX device [2], the FRC plasma produced in a quartz tube is translated to a metal confinement chamber in order to improve the accessibility to heating facilities (e.g., neutral beam injection [3], wave heating [4]).

The translation process is also important in relation

to many interesting phenomena, such as the spontaneous toroidal field generation [5], the shock wave formation at the reflection by the magnetic mirror and the rethermalization [6]. In those previous papers [5,6], the translation process was investigated by measuring the time evolution of the separatrix radius profile in the axial ( $z$ ) direction. Although the behavior of the FRC plasma during the translation in the  $x$ – $y$  plane perpendicular to the device axis is also important because of the frequent appearance of instabilities such as the  $n = 2$  rotational instability [1], the translation process in the  $x$ – $y$  plane has been scarcely investigated. For this purpose, computer tomography (CT) seems to be one of the most powerful techniques. However, only

*Corresponding author's e-mail: yosimura@ppl.eng.osaka-u.ac.jp*

*present address: <sup>1</sup> Nippon Television Network Corporation,*

*Tokyo 102-8004, Japan*

*<sup>2</sup> Toray Industries, Inc., Shiga 520-0842, Japan*

©2002 by The Japan Society of Plasma  
Science and Nuclear Fusion Research

a few experiments have so far employed the CT method in FRC plasma studies. In this study, we installed a CT system on the FIX device and measured firstly the behavior of the FRC plasma during the translation.

## 2. Experimental Apparatus

The FIX device consists of the formation region and the confinement region (Fig. 1). After the introduction of deuterium gas, the FRC plasma is produced by the theta pinch discharge in the formation region which consists of a quartz tube (2.0 m in length and 0.27 m in diameter) and theta pinch coils. Then, the FRC plasma is translated to the confinement region. The confinement region consists of the central straight section and the mirror field sections at both ends. The central section is composed of quasi-DC magnetic field coils and a metal vacuum chamber which acts as a flux conserver. The length and the diameter of the straight section are 3.4 m and 0.8 m, respectively. The strength of the quasi-DC magnetic field is  $B_z \approx 0.04$  T. The metal chambers of the mirror field sections are tapered and the strength of the magnetic mirror field is about 0.12 T. The typical line averaged electron density and pressure balance temperature (sum of the electron and ion temperatures) of translated FRC plasmas are  $\bar{n}_e \approx 5 \times 10^{19} \text{ m}^{-3}$  and  $T = T_e + T_i \approx 150$  eV, respectively. For the improvement of the confinement properties of the translated FRC plasma, axial compression coils are mounted coaxially with the device axis at the upstream side of the central straight section (Fig. 1). The compression coils produce the magnetic field of 0.1 T with the rise time of 34  $\mu\text{sec}$ . The axial compression of the FRC plasma is performed by energizing the segmented compression coils successively with time in such a way as to shorten the length of the plasma [7]. The time evolution of the separatrix radius,  $r_s$ , of the FRC plasma during the translation and the axial compression can be obtained by the excluded flux measurement using magnetic probes installed just inside the metal chamber wall on the assumption that the magnetic field lines are straight [8,9].

In order to observe the reflection of the FRC plasma by the magnetic mirror in the translation process, the CT system is installed at a distance of 1.2 m downstream side from the center of the confinement region (Fig. 1). This CT system is composed of three detector arrays installed to surround the plasma cross section (Fig. 2). Each array consists of a pinhole, an optical glass filter and two pieces of a photodiode array (HAMAMATSU-S5668-02). The photodiode array con-

sists of 16 elements of p-n photodiode having the active area of  $1.175 \text{ mm} \times 2.0 \text{ mm}$  with 1.575 mm pitch on a compact base with the dimensions of  $25.4 \text{ mm} \times 20.0 \text{ mm}$ . The spectral response range is  $\lambda = 320 \sim 1100 \text{ nm}$  and the peak sensitivity wavelength is  $\lambda_p = 960 \text{ nm}$ . The optical filter passes the light above 720 nm. Consequently, the sensitive spectral range of this CT system is  $\lambda = 720 \sim 1100 \text{ nm}$ , that is, the near-infrared region. Thus this system is insensitive to the spectral lines from deuterium atoms and strong impurity lines in the visible and ultraviolet regions. The rise time of the photodiode is 0.1  $\mu\text{sec}$ . The output current of each photodiode is converted to voltage by the preamplifier. Each voltage signal is amplified by the main amplifier and then digitized every 1  $\mu\text{sec}$  by the A/D converter. The total number of photodiodes used in the present experiment is  $18 \times 3 = 54$  because of the limited channel number of the data acquisition system. To avoid the light reflection at the vacuum wall, black anodized

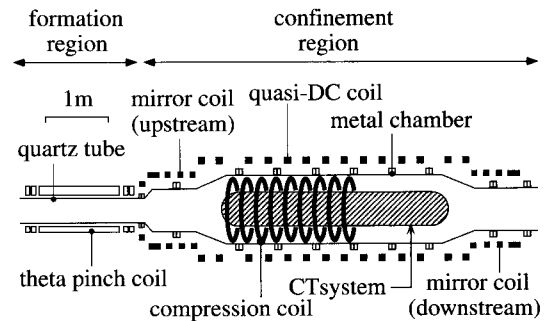


Fig. 1 Schematic drawing of the FIX device. The hatched region represents the translated FRC plasma.

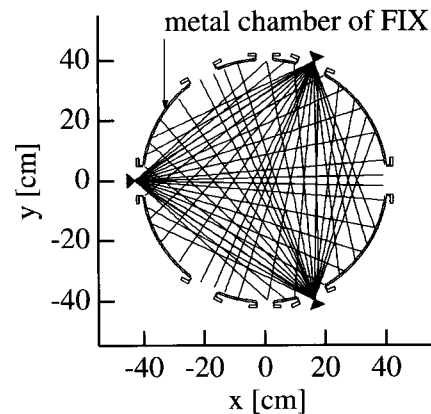


Fig. 2 Arrangement of viewing chords of photodiode detectors of three arrays on the FIX device.

aluminum panels are installed just inside the metal chamber of FIX. The Fourier-Bessel expansion technique [10] is employed to reconstruct two-dimensional distributions of the light emissivity of the FRC plasma in the  $x$ - $y$  plane perpendicular to the device axis. The highest reconstructable Fourier mode number,  $n$ , is limited by the number of the detector arrays installed at the same cross section. In the present case, we install three detector arrays on FIX in order to reconstruct up to  $n = 2$ , because the  $n = 2$  rotational instability is sometimes observed in FRC plasmas.

### 3. Results of Measurement

The typical temporal evolution of a translated FRC plasma is shown in Fig. 3. Figure 3(a) shows the time evolution of the  $r_s$  at the axial section of the CT system. The FRC plasma produced in the formation region is translated to the confinement region at about  $130\mu\text{sec}$ . At the time (1), marked by the arrow in Fig. 3(a), the FRC plasma is moving along the device axis. The temporal evolution of the separatrix radius profile in the axial direction,  $r_s(z)$ , shows that the peak of the  $r_s(z)$  reaches the mirror field region at the time (2) and the

FRC plasma is reflected by the mirror field of downstream side [6]. Next, the FRC plasma bounces back and after the time (3) it settles down in the confinement region. Then, the  $r_s$  decreases gradually [time (4)] and becomes zero at  $340\mu\text{sec}$  in the case without the axial compression, as shown in Fig. 3(a) by the dashed line. In the case with the axial compression the  $r_s$  increases again [time (5)] and reaches the maximum at the time (6).

Figures 3(b)–3(e) show the time evolution of the photodiode signals. Figure 3(b) is a signal of a photodiode whose viewing chord passes through the center of the plasma. On the contrary, Fig. 3(e) corresponds to the signal along the periphery of the plasma. The photodiode signals begin to rise just after the entrance of the FRC plasma to the confinement region. The signal of the photodiode viewing the plasma center [Fig. 3(b)] reaches the maximum at the time (2). Then, it begins to decrease earlier than the decrease of the  $r_s$ . By the application of the axial compression, the photodiode signals slightly increase again, as shown in Figs. 3(b)–3(e).

Figures 4(1)–4(6) show the reconstructed two-

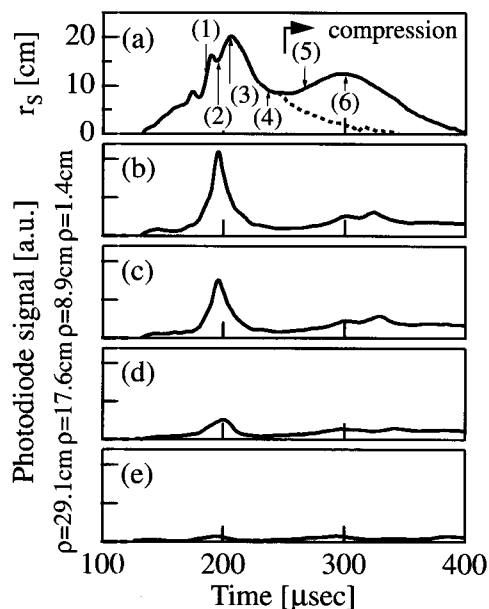


Fig. 3 The temporal evolution of (a) the separatrix radius,  $r_s$ , at the axial section of the computer tomography system and (b)–(e) photodiode signals. Here,  $\rho$  is the chord impact parameter relative to the center of the FIX device. In the figure (a), the  $r_s$  of the cases with and without the axial compression are shown by the solid and the dashed lines, respectively.

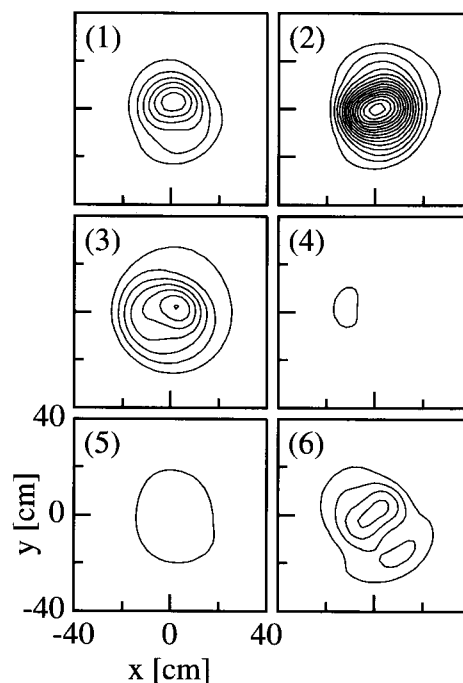


Fig. 4 Figures (1)–(6) show the two-dimensional distributions of the light emissivity of a translated FRC plasma at the time marked by arrows (1)–(6) in Fig. 3(a).

dimensional distributions of the light emissivity of the FRC plasma at the time marked by arrows (1)–(6) in Fig. 3(a). In Fig. 5(b), the time evolution of the peak intensity,  $I_{\text{peak}}$ , of the reconstructed emission profile during the translation is shown. Figure 5(c) indicates the temporal evolution of the half of the full width at half-maximum of the emission profile,  $r_{\text{emission}}$ . Figures 5(a) and 5(c) show that the  $r_s$  and  $r_{\text{emission}}$  are increasing at the time (1). At about 190  $\mu\text{sec}$  they reach the maximum because the peak of the  $r_s(z)$  arrives at the axial section of the CT system. Then, the peak of the  $r_s(z)$  passes over the axial section of the CT system and the  $r_s$  and  $r_{\text{emission}}$  decrease until the time (2). The contour maps of the emission are nearly symmetric around the center of the plasma at the time (1) [Fig. 4(1)] and the time (2) [Fig. 4(2)]. Figure 5(b) shows that the  $I_{\text{peak}}$  reaches the maximum when the FRC plasma is reflected by the mirror field of downstream side at the time (2). The reason why the  $I_{\text{peak}}$  reaches the maximum at the time (2) is not confirmed. However, the increment of the pressure balance temperature due to the rethermalization [6] is one of possible causes for it. After that, the  $I_{\text{peak}}$  begins to decrease, whereas the  $r_s$  and  $r_{\text{emission}}$  [Figs. 5(a) and 5(c)] increase again, reflecting the fact that the FRC plasma bounces back after the time (2) and the peak of the  $r_s(z)$  passes through the axial section of the CT system. About 10  $\mu\text{sec}$  after the reflection [time (3)] the  $r_s$  reaches the maximum [Fig. 5(a)] and the emission

profile becomes slightly non-symmetric near the center [Fig. 4(3)]. Then, the  $r_s$  begins to decrease [Fig. 5(a)]. Although the absolute value of the  $r_{\text{emission}}$  is not the same as that of the  $r_s$ , Figs. 5(a) and 5(c) show that the temporal evolution of the  $r_{\text{emission}}$  has the similar tendency to that of the  $r_s$  during the translation, indicating that the reconstructed emission profile represents the radiation not from the low temperature plasma outside the  $r_s$  but from the core plasma. Just after the axial compression [Fig. 4(5)], the intensity of the emission does not change so much as compared with that just before the axial compression [Fig. 4(4)]. However, after the rise time of the compression magnetic field the intensity of the emission increases again [Fig. 4(6)] and the  $r_s$  increases as well [Fig. 3(a)].

#### 4. Summary and Discussion

In the FIX device, the FRC plasma produced in a quartz tube is translated to a metal confinement chamber. A CT system for the investigation of the translation process of the FRC plasma was established. This system was composed of three arrays of detectors sensitive to the near-infrared radiation. To avoid the light reflection at the vacuum wall, black anodized aluminum panels were installed just inside the metal chamber. The Fourier–Bessel expansion technique was employed to reconstruct the two-dimensional distributions of the light emissivity of the FRC plasma. Our results showed that the intensity of the emission reached the maximum when the FRC plasma was reflected by the mirror field, and also that the temporal evolution of the width of the reconstructed emission profile had the similar tendency to that of the separatrix radius of the FRC plasma during the translation.

Although the impurity line radiation in the sensitive spectral range of this CT system remains to be assessed, the main component of the emission may be Bremsstrahlung, because the impurity line radiation emitted from the FRC plasma was very weak in the near-infrared region in the NUCTE device [11] where the FRC plasma was produced by the theta pinch discharge in the same way as in FIX. However, confirmation by the spectroscopic measurement is required in the confinement region of FIX. In addition, we are now planning to measure the detailed electron density profile by the five-chord interferometer and the electron temperature profile by the three-channel Thomson scattering apparatus. These measurement will help us to identify the relation between the emission profile and the profiles of the electron density and

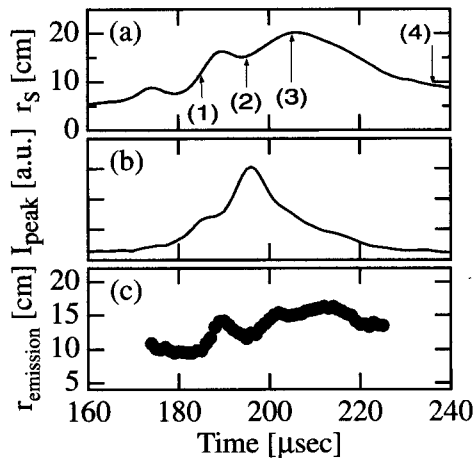


Fig. 5 The temporal evolution of (a) the separatrix radius,  $r_s$ , at the axial section of the computer tomography system, (b) the peak intensity of the emission profile,  $I_{\text{peak}}$ , and (c) the half of the full width at half-maximum of the reconstructed two-dimensional distribution of the FRC plasma,  $r_{\text{emission}}$ .

temperature.

In conclusion, this simple CT system will be useful for exploring the dynamics of the FRC plasma during the translation and the axial compression. The photodiode used in the present experiment can be modified to be sensitive enough to soft x-ray by removing the glass envelope on the active area of the photodiode. Therefore, this photodiode can be also used for the soft x-ray tomography of high temperature plasmas such as tokamaks. In fact, one of the authors installed a CT system consisting of five similar photodiodes on the WT-3 tokamak and it was used for the investigation of magnetohydrodynamic activities [12].

### References

- [1] M. Tuszewski, Nucl. Fusion **28**, 2033 (1988).
- [2] S. Okada *et al.*, Nucl. Fusion **41**, 625 (2001).
- [3] T. Asai *et al.*, Phys. Plasmas **7**, 2294 (2000).
- [4] K. Yamanaka *et al.*, Phys. Plasmas **7**, 2755 (2000).
- [5] A. Shiokawa *et al.*, Phys. Fluids B **5**, 534 (1993).
- [6] H. Himura *et al.*, Phys. Plasmas **2**, 191 (1995).
- [7] K. Kitano *et al.*, Phys. Plasmas **8**, 3630 (2001).
- [8] M. Tuszewski, Phys. Fluids **24**, 2126 (1981).
- [9] M. Tuszewski *et al.*, Rev. Sci. Instrum. **54**, 1611 (1983).
- [10] Y. Nagayama, J. Appl. Phys. **62**, 2702 (1987).
- [11] M. Urano *et al.*, J. Phys. Soc. Jpn **64**, 4077 (1995).
- [12] S. Yoshimura *et al.*, Phys. Plasmas **9**, 3378 (2002).